Title
CO_2 source inversions using satellite observations of the upper troposphere

Journal
Geophysical Research Letters, 28(24)

ISSN
00948276

Authors
Park, Bernard C
Prather, Michael J

Publication Date
2001-12-15

DOI
10.1029/2001GL013604

CO_2 source inversions using satellite observations of the upper troposphere

Bernard C. Pak and Michael J. Prather

Department of Earth System Science, University of California, Irvine

Abstract. Satellite observations of CO_2 abundance in the upper troposphere can provide a major constraint for deriving the net carbon fluxes from tropical landmasses that is unavailable from current surface observations. Such global CO_2 profiling with an uncertainty of about 1% (3 ppm) contains key longitudinal information needed to derive surface fluxes in a standard Bayesian inversion. Upper-tropospheric data available from flight-proven FTIR solar occultation measurements could provide comparable information to that from yet-to-be-demonstrated column CO_2 observations, which have heretofore been the focus of carbon cycle studies. A strategy for improving CO_2 source inversions with either type of satellite data should focus on tropical observations and on careful evaluation of possible sampling biases affecting the observational uncertainties.

Introduction

Satellite measurements of atmospheric CO_2 abundance are contemplated as a key extension to the current *in situ* surface measurements that – even without sampling key geographic regions – have still provided us with a global view of the carbon cycle. The surface sampling network [e.g., *GLOBALVIEW-CO_2*, 2000, and predecessors] has been used in inversion studies [e.g., *Enting et al.*, 1995; *Rayner et al.*, 1999; *Gurney et al.*, 2001] that constrain CO_2 fluxes and hence identify major source/sink regions. However, this sparse and spatially skewed network is not sufficient to constrain regional fluxes with the needed certainty. For instance, these surface measurements require the ocean and land biosphere to be a global net sink of about 3 Gt-C yr^{-1}, yet the error estimate in the Northern African flux alone is about 1 Gt-C yr^{-1} [*Gurney et al.*, 2001] . Although remote measurements of CO_2 abundance via satellite will not achieve the precision possible from *in situ* measurements, they can readily provide many observations with near-global coverage and with vertical information that is not possible from a surface network. Such data would greatly refine quantification of CO_2 fluxes in some regions, particularly the tropical continents.

The carbon cycle community has focused heretofore on column measurements of CO_2 from space since the signal in the column is dominated by the boundary layer and surface emissions/uptake. A recent study [*Rayner and O'Brien*, 2001] establishes the required observational uncertainty of the column-integrated CO_2 abundance to be useful in constraining surface fluxes. They apply Bayesian inversions on monthly-mean pseudo-observations (i.e., simulated with the forward atmospheric tracer model) and conclude that 8°x10° satellite footprints with a monthly uncertainty of 2.5 ppm (<1%) would rival a surface network of 56 stations in terms of error estimates in regional CO_2 fluxes.

As an alternative to column measurements, space- and balloon-borne measurement of atmospheric trace gases with Fourier-transform infrared (FTIR) observations have already demonstrated the capability of simultaneously measuring profile abundance of a wide suite of trace gases with relatively high precision and specificity [*Gunson et al.*, 1996; *Toon et al.*, 1999]. These FTIR solar occultations have the best signal-to-noise of almost any remotely sensed trace gas abundance and can provide vertical profiles from the stratosphere down to about 5 km altitude. This study shows that such profiles of CO_2 abundance with a monthly-mean uncertainty of about 1% (3 ppm) in the upper troposphere contain key longitudinal information and, in concert with the existing surface network, can greatly improve our derivation of the CO_2 fluxes from continental-scale regions, equal to or better than can be achieved with column measurements.

First, the approach is described, including the atmospheric tracer model, *a priori* flux data, and observed CO_2 data. Next, the Bayesian inversion results (*a posteriori* fluxes and error estimates) are compared for different combinations of pseudo-observations, namely a surface network, global column measurements, and upper tropospheric profiles for a typical occultation orbit. Finally, the issue of observational uncertainty and limitations of satellite measurements is discussed.

Approach

The Atmospheric Model is used to map fluxes from a given source region onto atmospheric abundance over the globe. These resulting response functions, relating fluxes at one time to abundance at all later times, form the core of the inversion method. The UC Irvine Chemistry-Transport Model (UCI-CTM) used here has a global resolution of 4° latitude by 5° longitude and 9 vertical levels from the surface to the lower stratosphere. The circulation is taken from a year of the GISS II' general circulation model [*Koch and Rind*, 1998]. Tracer transport includes winds, vertically resolved convective fluxes and boundary-layer turbulent mixing, while preserving the second-order moments of the tracer distribution within each grid cell [*Prather*, 1986]. The model's characteristics are well documented [*Prather et al.*, 1987; *Wild and Prather*, 2000] and the UCI-CTM or its progenitors have participated in the international CTM comparisons [*Jacob et al.*, 1997; *Rasch et al.*, 2000; *Ehhalt and Prather*, 2001] and CO_2 comparisons (TransCom3: phase 3 of the Transport Model Intercomparison Project [*Gurney et*

Paper number 2001GL013604.
0094-8276/01/2001GL013604$05.00

Table 1. *A priori* and *a posteriori* CO_2 flux errors (all one-sigma in Gt-C yr^{-1}) for the 22 source regions. *A priori* fluxes and uncertainties are from TransCom3. *A posteriori* fluxes derived here (not shown) equal *a priori* fluxes within the quoted errors. Retrievals use combinations of pseudo-observations (with their monthly uncertainties): S = surface network (GLOBALVIEW uncertainties, 0.13 to 15 ppm), C = column integrated (3 ppm), and P = free-troposphere (3 ppm).

	Net	*A priori*		*A*	*posteriori*	**errors**		
	flux	**uncertainties**	**S**	**C**	**P**	**S+C**	**S+P**	**S+C+P**
Total	3.91	±9.38	±1.56	±1.79	±1.87	±1.18	±1.19	±1.07
Land								
Boreal N America	0.01	±2.00	±0.22	±0.41	±0.48	±0.20	±0.21	±0.19
Temperate N America	1.46	±2.00	±0.34	±0.41	±0.42	±0.29	±0.30	±0.27
Tropical America	0.11	±2.00	±0.48	±0.32	±0.32	±0.28	±0.28	±0.23
S America	0.11	±2.00	±0.43	±0.40	±0.41	±0.35	±0.35	±0.31
N Africa	0.09	±2.00	±0.50	±0.29	±0.27	±0.25	±0.23	±0.20
S Africa	0.11	±2.00	±0.38	±0.27	±0.26	±0.22	±0.21	±0.18
Boreal Eurasia	0.16	±2.00	±0.32	±0.39	±0.46	±0.27	±0.29	±0.26
Temperate Eurasia	1.67	±2.00	±0.41	±0.39	±0.40	±0.30	±0.30	±0.27
SE Asia	0.32	±2.00	±0.48	±0.37	±0.35	±0.31	±0.30	±0.26
Australasia	0.07	±2.00	±0.16	±0.38	±0.40	±0.15	±0.15	±0.15
Europe	1.53	±2.00	±0.36	±0.41	±0.46	±0.31	±0.33	±0.30
Ocean								
N Pacific	-0.28	±2.00	±0.25	±0.40	±0.41	±0.20	±0.21	±0.19
W Pacific	0.17	±2.00	±0.27	±0.32	±0.31	±0.22	±0.22	±0.19
E Pacific	0.47	±2.00	±0.23	±0.31	±0.31	±0.18	±0.18	±0.16
S Pacific	-0.22	±2.00	±0.29	±0.42	±0.43	±0.26	±0.26	±0.24
Northern Ocean	-0.39	±2.00	±0.23	±0.44	±0.50	±0.22	±0.22	±0.21
N Atlantic	-0.20	±2.00	±0.25	±0.40	±0.41	±0.21	±0.22	±0.20
Tropical Atlantic	0.14	±2.00	±0.33	±0.33	±0.32	±0.24	±0.23	±0.20
S Atlantic	-0.13	±2.00	±0.40	±0.46	±0.47	±0.35	±0.36	±0.34
Southern Ocean	-0.89	±2.00	±0.15	±0.39	±0.45	±0.14	±0.14	±0.13
Trop Indian Ocean	0.15	±2.00	±0.31	±0.35	±0.33	±0.25	±0.24	±0.21
S Indian Ocean	-0.55	±2.00	±0.22	±0.46	±0.47	±0.21	±0.21	±0.20

al., 2000]). The model response functions are derived for a set of specified CO_2 flux patterns from the TransCom3 protocol: (i) fossil-fuel flux patterns for 1990 [*Andres et al.*, 1996] and 1995 [*Brenkert*, 1998], (ii) a global biosphere with large, realistic seasonal variations but no net CO_2 fluxes [*Randerson et al.*, 1997], (iii) monthly mean ocean fluxes derived from sea-surface pCO_2 [*Takahashi et al.*, 1999], and (iv) a unit flux from each of 22 regions that represent the unknown fluxes in the inversions (Table 1; see Figure 1 in *Gurney et al.* [2001]).

A Priori Flux Data provide one set of constraints. Inversions with a limited set of atmospheric observations (almost always the case) are often under-determined. To overcome this problem, the *a priori* fluxes serve as a first-guess for each region being solved for, and the corresponding *a priori* uncertainties then constrain the derived *a posteriori* fluxes within a reasonable range. These *a priori* data on fluxes and their one-sigma uncertainties are usually based on bottom-up studies of fluxes for each region. The *a priori* fluxes and uncertainties for the 22 regions here (Table 1) are taken from the TransCom3 Level-2 experiment.

The Observational Data provide another set of constraints in the inversion. The observations with their one-sigma uncertainties would nominally be taken from atmospheric measurements of CO_2 abundance. In this feasibility study, however, we assess the relative values of yet-to-be-made satellite observations and thus generate pseudo-observations from forward simulations of the atmospheric model using the input data as the true fluxes. At first this may seem a tautology since the inversion can of course readily retrieve these fluxes. It is the *a posteriori* error estimates, however, that are the foci here. As evident from Equation 1 (in inversion methodology section below), these errors do not significantly change when either random noise within the prescribed uncertainty is added to the pseudo-observations or slightly different *a priori* fluxes are used in the inversion. (In sensitivity tests, the retrieved *a posteriori* fluxes in both cases are notably different from the control.) With this approach, we inherently assume that atmospheric tracer models will become increasingly realistic and no longer a large part of the estimated errors. This may seem optimistic in that *Gurney et al.* [2001] show that model-model differences (interpreted as CTM error) contribute equally with lack of observations to the *a posteriori* errors, but this study included a wide range of old and new models as well as mixtures of assimilated and climate-model meteorology, exaggerating the true model error.

Three Pseudo-observation Data Sets are created by sampling the atmospheric model simulation of CO_2 at specified grid cells. For the surface network, *Case S* samples the grid cell containing the measurement site, except some coastal stations that select for clean marine air are sampled at the upwind full-ocean grid cell. TransCom3 selected 76 surface stations with the best long-term records for the Level-1 experiment (see Figure 1 in *Gurney et al.* [2001]). The uncertainties in surface network observations are based on the analysis of the real CO_2 measurements at these sites: generally 0.13 to 4.9 ppm, except for 3 special sites in the vicinity of large sources/sinks, e.g., 15 ppm at a northern continental flux tower. *Case S* pseudo-observations are saved as monthly

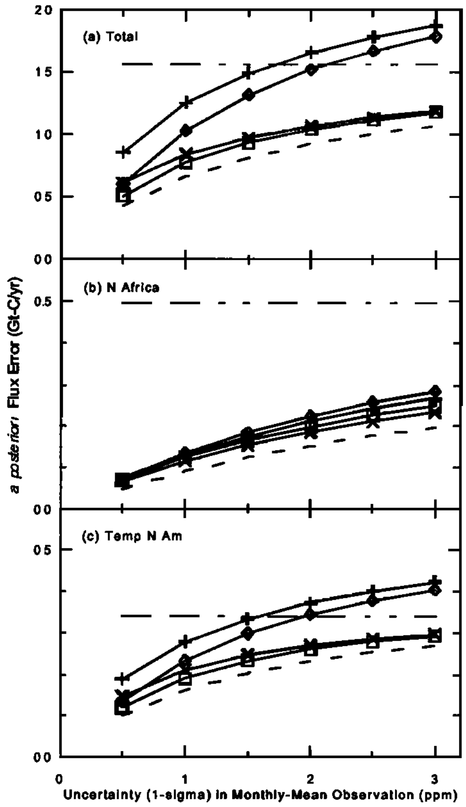

Figure 1. Error estimates of the predicted net CO_2 fluxes (Gt-C yr^{-1}) as a function of uncertainty in the pseudo-observations (one-sigma in ppm). Shown are (a) Total (square root of the sum of the squared errors from the 22 regions), (b) Northern Africa region, and (c) Temperate North America region. Lines refer to different combinations of data sets: S (dash-dot), C (solid, diamonds), P (solid, pluses), S+C (solid, boxes), S+P (solid, Xs), S+C+P (dotted).

means over the entire grid cell with no pollution events removed. For the satellite columns, *Case C* assumes global coverage from polar orbiters providing monthly means at 4°x5° (latitude-by-longitude) grid cells (2545 columns with some polar aggregation). The true spatial resolution achievable as monthly mean columns is uncertain since the footprint of each measurement is likely much smaller than this grid and clouds would obscure a large fraction of possible measurements. An important issue in uncertainty of column observations is the averaging of the limited, clear-sky measurements to produce an unbiased monthly average over the entire grid cell. Such uncertainty is not simply the measurement precision divided by the square root of the number of measurements. For satellite profiling, *Case P* considers the unusual sampling geometry and frequency of observations possible with solar occultation spectroscopy. By its nature, a solar occultation instrument can retrieve average CO_2 concentrations in a stretch of air about 400 km across and 2 km thick, a resolution comparable to that of current CTMs. Such free troposphere measurements are far less biased in terms of possible systematic sampling errors (e.g., clouds, diurnal cycles in emissions) than are column measurements. Each measurement is represented here by pseudo-observation in one of our 4°x5° model grid cell at a certain model level. An optically thick cloud in that cell will result in the loss of that particular pseudo-observation. With an orbital inclination of 48° there is moderately uniform sampling (about 30 profiles per day) from about 60°S to 60°N with a repeat cycle of 25 days. Thus for *Case P* we generate pseudo-observations for 360 vertical profiles, assuming about half of the possible profiles are lost due to cloudy conditions. The vertical profiles consist of sampling at 11, 8 and 5 km altitudes (model levels 7-6-5) with a further loss of half the 5-km data to clouds. In *Case P*, there is reduced observational uncertainty (compared with *Case C*) in determining the spatial average of a grid cell from a single measurement, but greater uncertainty due to the fewer measurements used to determine the monthly average. The observational uncertainty of satellite CO_2 observations is not easy to predict, and for *Cases C* and *P* we consider a range from 3 to 0.5 ppm.

Inversions and Sensitivity Studies

The Bayesian inversion methodology is outlined in *Enting et al.* [1995] and *Rayner et al.* [1999]. We take the atmospheric model response functions (A), the *a priori* fluxes and uncertainties (F), and a particular set of pseudo-observations with uncertainties (O). We then derive the *a posteriori* fluxes (not of interest here) and their estimated errors E (equation (1), based on *Tarantola* [1987]). All inversions here are the equivalent of Level-2 in the TransCom3 protocol and hence use monthly-mean observations. The estimated flux errors for each of the 22 regions using 3 ppm observational uncertainties are shown in Table 1 for six different sets of pseudo-observations: S, C, P, S+C, S+P, and S+C+P.

$$E = (A^T O^{-1} A + F^{-1})^{-1} \tag{1}$$

where E = uncertainty covariance matrix of estimated fluxes, A = response function from transport model, O = uncertainty covariance matrix of observations, F = uncertainty covariance matrix of prior fluxes.

Generally, due to under-observation by the surface network, most land regions have larger *a posteriori* errors than do oceanic regions, see Table 1 column S. Hence we expect the satellite observations to yield the greatest improvement in deriving continental fluxes of CO_2. Indeed, the addition of the satellite observations with uncertainties of 3 ppm (columns S+C or S+P) shows negligible reduction in *a posteriori* errors over oceanic regions (30% for Tropical Atlantic and 5-20% for others) while yielding large reductions of 40-50% over the tropical landmasses of Africa, Asia, and the Americas. Not unexpectedly, the profile data with no observation poleward of 60° do not improve the high-latitude flux errors, but surprisingly the column data with full global coverage also fail to do so. One can only conclude that the surface network does an adequate job for the high-latitude regions and much smaller uncertainties in the satellite data (<1 ppm) are needed to significantly reduce errors in the CO_2 fluxes worldwide. The dependence on the uncertainty of the satellite data is shown in Figure 1, where the flux errors are calculated for a range of observational uncertainties from 0.5 to 3 ppm. The Total value (panel a) is the square root of the summed squared errors from all 22 regions. The individual regions of North Africa (panel b) and Temperate North America (panel c) are typical for tropical and mid/high-latitude landmasses, respectively. In the Tropics satellite data with uncertainties of 3 ppm show dramatic improvements; whereas in mid/high-latitudes the data show marginal improvements unless the uncertainties are 1 ppm or less (<0.3%). Column and profile observations, as defined here and over a wide range of uncertainties, yield nearly identical benefits for all regions, but combining the two shows negligible improvement (column S+C+P).

This study is comparable to that of *Rayner and O'Brien* [2001], who derive only the equivalent of our curves S and C from Figure 1a and do not look at the relative improvement when satellite data are added to the surface data (S+C). Their results are consistent with those here: their cross-over point (2.5 ppm) is slightly larger than ours (2.2 ppm), which could be due to differences in atmospheric model, choice of surface stations, and input fluxes. The similar results support the robustness of both analyses and re-confirm the importance of achieving uncertainties of <1% in the mean observations from satellite.

Sensitivity to the pseudo-observations is investigated by adding random noise (within the specified uncertainty) to this data. The predicted *a posteriori* fluxes change significantly (within the *a posteriori* errors), but their error estimates do not. This exercise re-emphasizes the importance of (i) the observations representing the space-time average of what the response function simulates and (ii) the uncertainties including possible systematic biases.

Sensitivity to observational resolution is investigated by degrading the 4°x5° pseudo-observations of *Case C* to 4°x10° (1302 columns), 8°x10° (666 columns), and the limited 360 columns of *Case P*. The *a posteriori* errors decrease less than linearly with increased resolution, close to logarithmic. It follows that, when improved computing resources make 1°x1° CTMs commonplace, matching improvement in observations may halve the present error estimates from the 4°x5° model.

Conclusions

Incorporating satellite with surface observations can clearly improve our understanding of net carbon fluxes from large geographic regions by reducing the *a posteriori* flux errors. Free tropospheric abundances at coarse spatial resolution are comparable to more highly resolved column abundances of CO_2. Improvements are greatest over tropical landmasses, where observational uncertainties of even 3 ppm in either data set would reduce flux errors by half. Satellite data is much less useful over high latitudes in either hemisphere where uncertainties of less than 1 ppm would be needed to show notable improvements. Indeed a satellite strategy probably needs to emphasize low-latitude observations to have the greatest payoff.

Vertical profiles of CO_2 abundance in the free troposphere from solar occultation with a full spectrum FTIR have the added advantage of retrieving abundance of more than 30 other trace gases and aerosols in the same air mass as the CO_2. Such observations combined with a multi-species inversion could further reduce the uncertainty in CO_2 fluxes. Nevertheless, an unresolved concern here is the spatial and temporal representativeness of such satellite observations and how, combined with the individual measurement precision, they are incorporated into the observational uncertainties used in the inversion.

Acknowledgments. UCI tracer model development is funded by the atmospheric chemistry programs of NASA and NSF. The authors want to thank the TransCom3 group, especially K. Gurney, R. Law, P. Rayner and S. Denning for setting up the protocol and the inversion codes.

References

Andres, R. J., G. Marland, I. Fung, and E. Matthews, A 1°×1° distribution of carbon dioxide emissions from fossil fuel consumption and cement manufacture, 1950-1990, *Global Biogeochem. Cycles*, *10*, 419–429, 1996.

Brenkert, A. L., Carbon dioxide emission estimates from fossil-fuel burning, hydraulic cement production, and gas flaring for 1995 on a one degree grid cell basis, 1998, [Available at http://cdiac.esd.ornl.gov/ndps/ndp058a.html].

Ehhalt, D., and M. J. Prather, Chapter 4. Atmospheric Chemistry and Greenhouse Gases, in *Climate Change 2001: The Scientific Basis*, pp. 239–287, Cambridge U. Press, 2001.

Enting, I. G., C. M. Trudinger, and R. J. Francey, A synthesis inversion of the concentration and $\delta^{13}C$ of atmospheric CO_2, *Tellus*, *47B*, 35–52, 1995.

GLOBALVIEW-CO_2, Cooperative Atmospheric Data Integration Project - Carbon Dioxide, CD-ROM, NOAA CMDL, Boulder, Colorado, 2000, [Also available at ftp.cmdl.noaa.gov/ccg/co2/GLOBALVIEW].

Gunson, M. R., et al., The Atmospheric Trace Molecule Spectroscopy (ATMOS) experiment: Deployment on the ATLAS Space Shuttle missions, *Geophys. Res. Lett.*, *23*, 2333–2336, 1996.

Gurney, K., R. Law, P. Rayner, and A. S. Denning, Transcom 3 experimental protocol, *Department of atmospheric science, colorado state university, USA, paper no. 707*, 2000.

Gurney, K. R., et al., Robust regional estimates of annual mean CO_2 sources and sinks, *Nature*, 2001, (submitted).

Jacob, D. J., et al., Evaluation and intercomparison of global atmospheric transport models using ^{222}Rn and other short-lived tracers, *J. Geophys. Res.*, *102*, 5953–5970, 1997.

Koch, D., and D. Rind, $^{10}Be/^{7}Be$ as a tracer of stratospheric transport, *J. Geophys. Res.*, *103*, 3907–3917, 1998.

Prather, M., Numerical advection by conservation of second-order moments, *J. Geophys. Res.*, *91*, 6671–6681, 1986.

Prather, M., M. McElroy, S. Wofsy, G. Russell, and D. Rind, Chemistry of the global troposphere: Fluorocarbons as tracers of air motion, *J. Geophys. Res.*, *92*, 6579–6613, 1987.

Randerson, J. T., M. V. Thompson, T. J. Conway, I. Y. Fung, and C. B. Field, The contribution of terrestrial sources and sinks to trends in the seasonal cycle of atmospheric carbon dioxide, *Global Biogeochem. Cycles*, *11*, 535–560, 1997.

Rasch, P. J., et al., A comparison of scavenging and deposition processes in global models: results from the WCRP Cambridge Workshop of 1995, *Tellus*, *52B*, 1025–1056, 2000.

Rayner, P. J., and D. M. O'Brien, The utility of remotely sensed CO_2 concentration data in surface source inversions, *Geophys. Res. Let.*, *28*, 175–178, 2001.

Rayner, P. J., I. G. Enting, R. J. Francey, and R. L. Langenfelds, Reconstructing the recent carbon cycle from atmospheric CO_2, $\delta^{13}C$ and O_2/N_2 observations, *Tellus*, *51B*, 213–232, 1999.

Takahashi, T., et al., Net sea-air CO_2 flux over the global oceans: An improved estimate based on the sea-air pCO_2 difference, in *Extended abstracts of the 2nd International CO_2 in the Oceans Symposium, Tsukuba, Japan, January 18-22, 1999*, pp. 18–01, 1999.

Tarantola, A., *Inverse Problem Theory: Methods for Data Fitting and Parameter Estimation*, Elsevier, Amsterdam, 1987.

Toon, G. C., et al., Comparison of MkIV balloon and ER-2 aircraft measurements of atmospheric trace gases, *J. Geophys. Res.*, *104*, 26,779–26,790, 1999.

Wild, O., and M. J. Prather, Excitation of the primary tropospheric chemical mode in a global three-dimensional model, *J. Geophys. Res.*, *105*, 24,647–24,660, 2000.

B. C. Pak and M. J. Prather, Department of Earth System Science, University of California, Irvine, CA 92697-3100. (email: bpak@uci.edu)

(Received June 8, 2001; revised September 20, 2001; accepted October 3, 2001.)